JOURNAL OF CATALYSIS **116**, 399–406 (1989)

V_2O_5–SiO_2-Catalyzed Methane Partial Oxidation with Molecular Oxygen

NICHOLAS D. SPENCER AND CARMO J. PEREIRA

Research Divison, W. R. Grace & Company, 7379 Route 32, Columbia, Maryland 21044

Received August 19, 1988; revised November 15, 1988

The partial oxidation of methane to formaldehyde by molecular oxygen has been studied using vanadium(V) oxide–silica catalysts in the temperature range 773–873 K at 1 atm pressure. Although HCHO selectivity in excess of 70% was observed at very low conversions, it was found to decrease rapidly as the extent of reaction was increased. At the highest conversions studied (6.4%), carbon monoxide was the principal reaction product. Methane oxidation was found to follow a sequential reaction path, where formaldehyde is formed from methane, carbon monoxide from formaldehyde, and carbon dioxide from carbon monoxide. This is in contrast to the molybdenum(VI) oxide–silica-catalyzed reaction, where CO_2 is formed directly from methane in a parallel pathway. A model has been constructed based on the sequential mechanism and experimentally derived kinetic parameters. It accounts for the observed selectivity and conversion behavior of this catalyst.

INTRODUCTION

Formaldehyde is currently manufactured from methane via syngas and methanol (*1–3*). A process for the production of formaldehyde directly from methane would potentially reduce both capital and operating costs, and therefore be of considerable industrial importance. Until recently, however, high selectivities to formaldehyde have been achievable only by using nitrous oxide as an oxidant (*4–6*).

Recently, we reported (*7, 8*) that MoO_3–SiO_2 catalyzed the reaction of CH_4 with O_2 to form HCHO. Kinetic analysis indicated that the methane is directly oxidized to CO_2 and HCHO, with HCHO being further oxidized to CO. High HCHO selectivities were observed at low CH_4 conversions and HCHO selectivity decreased monotonically with increasing conversion. Another observed trend was that the HCHO selectivity increased with increasing temperature at a fixed CH_4 conversion. Unfortunately, at temperatures above 923 K and high CH_4 conversions, selectivity to HCHO continued to increase only slightly, presumably due to the onset of undesirable side reactions (such as gas-phase HCHO oxidation, $CO \rightarrow CO_2$, and the water–gas shift reaction).

Although references to the partial oxidation of methane over V_2O_5–SiO_2 exist in the patent literature (*6, 9*), there are few papers on the subject. Zhen *et al.* (*5*) found that V_2O_5–SiO_2 catalyzed the reaction when N_2O was used as an oxidant, producing methanol and formaldehyde in high selectivities. In the present work, the V_2O_5–SiO_2-catalyzed partial oxidation of CH_4 has been studied using molecular oxygen. A kinetic model that describes the conversion and selectivity for V_2O_5–SiO_2 catalysts has been proposed. The kinetic parameters obtained are compared with those previously obtained for the MoO_3–SiO_2 system and it is shown that V_2O_5–SiO_2 is the more active catalyst. However, there appear to be important differences in the mechanisms operating in the two systems.

METHODS

The V_2O_5–SiO_2 catalysts were prepared from ammonium metavanadate and silica. The silica sources were either Cabosil M5 (a fumed silica manufactured by Cabot

0021-9517/89 $3.00

Corp.) or "ID" silica gel (manufactured by the Davison Chemical Division of W. R. Grace & Co.) The latter was washed in a stream of dilute sulfuric acid (pH 3) at 373 K to reduce the sodium level. When it was washed for several days, the sodium level in the silica was reduced to 20 ppm, and this material is referred to as "acid-washed silica gel" (AWSG). V_2O_5–AWSG catalysts were prepared by slurrying the gel with ammonium metavanadate solution and evaporating to dryness. This was followed by calcination at 873 K for several hours. V_2O_5–Cabosil catalysts were prepared by incipient wetness impregnation, followed by drying and calcination. Vanadium and sodium analyses of the catalysts were carried out by atomic absorption spectroscopy. Prior to use, catalysts made from Cabosil were compressed at 15,000 psi and crushed, and all catalysts were screened to a particle size of 0.5–0.7 mm. Properties of the screened catalysts are summarized in Table 1.

Small samples of catalysts (0.2 g) were tested at atmospheric pressure in a quartz flow microreactor with gas chromatographic detection of products. The apparatus has been described in detail elsewhere (*7*). A methane–oxygen mixture was passed at 1 atm over the catalyst at gas hourly space velocities ranging from 1000 to 20,000 h^{-1} (at NTP). Due to the highly exothermic nature of methane oxidation, great care was exercised to minimize nonisothermal effects. The catalyst temperature was varied from 773 to 873 K.

Formaldehyde oxidation experiments were carried out by passing an argon–oxygen (10% O_2) mixture through a thermostated bubbler containing paraformaldehyde. In this way, steady-state, gas-phase HCHO concentrations of 0.7 vol% could readily be fed into the reactor and over the same catalyst bed that was used for the methane oxidation experiments. A constant space velocity of 5000 h^{-1} (NTP) was used and the temperature was varied from 443 to 873 K.

TABLE 1

Properties of Catalysts Used in the Present Study

Description	wt% V	BET surface area (m^2 g^{-1})	[Na] (ppm)
V_2O_5–AWSG	1.3	277	26
V_2O_5–Cabosil	1.1	210	<4

RESULTS

The principal products of methane oxidation were found to be formaldehyde, carbon monoxide, carbon dioxide, and water. Methanol and hydrogen were detected in trace quantities. Substituting quartz chips for the catalyst resulted in negligible methane conversion over the range of operating conditions described above. This suggests that gas-phase reactions are not significant in this study. When AWSG was used as a catalyst, slight methane conversion was detected. AWSG appears to be approximately two orders of magnitude less active than V_2O_5–AWSG, and these results are discussed in detail elsewhere (*7*).

Reactor effluent data obtained using V_2O_5–AWSG under varying operating conditions have been plotted in the form of product selectivity (i.e., the percentage of product in the converted methane) vs percentage methane conversion. As shown in Fig. 1a, the formaldehyde selectivity decreases monotonically with increasing methane conversion. High formaldehyde selectivities are observed at low methane conversion, indicating that formaldehyde is a primary product. At a given level of methane conversion, formaldehyde selectivity increases with increasing temperature. Selectivity to carbon monoxide tends to zero at zero methane conversion and increases with methane conversion, implying that carbon monoxide is a secondary product (Fig. 1b). The selectivity to carbon dioxide also tends to zero at zero methane conversion, implying that carbon dioxide is also a

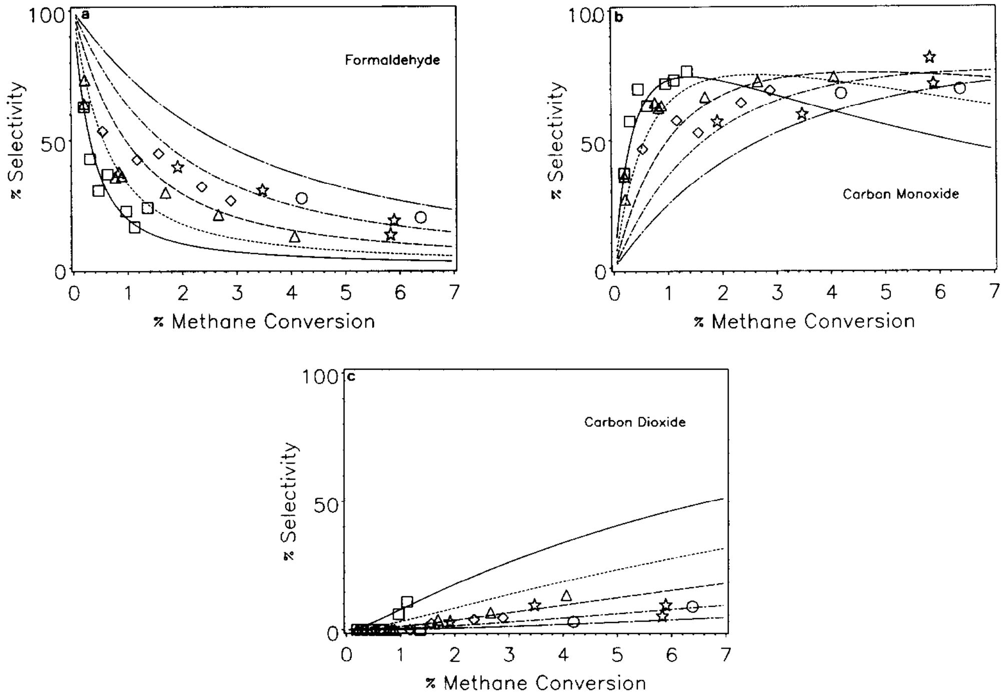

FIG. 1. Selectivity vs methane conversion curves. Symbols correspond to data; lines correspond to model predictions (□— 773 K, △ --- 798 K, ◇--- 823 K, ☆--- 848 K, ○ —-— 873 K).

secondary product (Fig. 1c). No change in conversion or selectivity behavior was detected when the methane-to-oxygen ratio was varied between 28 : 1 and 10 : 1, providing that oxygen conversion was kept below 100%. This strongly suggests that the reaction is zero order in oxygen, as is the case with several other hydrocarbon partial oxidation reactions (*8, 10, 11*). Very similar selectivity behavior was observed with the V_2O_5–Cabosil and V_2O_5-AWSG of comparable V_2O_5 loadings.

Formaldehyde oxidation results, shown in Fig. 2, indicate that carbon monoxide and carbon dioxide are the only significant reaction products. At low conversion, carbon monoxide is the only product observed. As the conversion of formaldehyde is increased, the carbon monoxide concentration increases and reaches a maximum concentration at ≈800 K, as formaldehyde conversion nears 100% and carbon dioxide production becomes more significant. These results suggest that carbon monoxide is a primary product and carbon dioxide is a secondary product of the formaldehyde oxidation reaction, consistent with the results discussed above.

The above results indicate that, in the

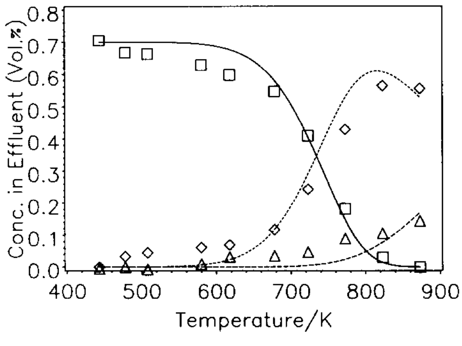

FIG. 2. Product gas distribution during oxidation of HCHO. Symbols correspond to data; lines correspond to model predictions (□— HCHO, ◇--- CO, △– – – CO_2).

V_2O_5–SiO_2 system, carbon dioxide forms via the sequence

$$CH_4 \rightarrow HCHO \rightarrow CO \rightarrow CO_2.$$

This suggests the overall reaction scheme

$$CH_4 + O_2 \xrightarrow{k_1} HCHO + H_2O$$

$$HCHO + \tfrac{1}{2}O_2 \xrightarrow{k_2} CO + H_2O$$

$$CO + \tfrac{1}{2}O_2 \xrightarrow{k_3} CO_2$$

The relationship between the various species and reactor conditions for a reaction that is first order in methane concentration and zero order in oxygen concentration in an isothermal, plug-flow reactor is

$$\ln\left[1 - \frac{c_{HCHO} + c_{CO} + c_{CO_2}}{c^0_{CH_4}}\right] = -\frac{k_1}{GHSV} \quad (1)$$

where c is the mole fraction, GHSV is the gas hourly space velocity at reaction conditions, and k_1 is the reactor-volume-based rate constant for the HCHO formation reaction.

The left-hand side of Eq. (1) is plotted vs 1/GHSV in Fig. 3. The resulting straight lines confirm that the methane is being oxidized in a first-order reaction. The slope of each line corresponds to $-k_1$ at that particular temperature, enabling us to construct an Arrhenius plot (Fig. 4). The Thiele modulus was calculated and the methane oxidation reaction was found to be kinetically controlled and not limited by intraparticle diffusion over the temperature range examined. For example, at the highest methane conversion examined [873 K and space velocity of 10,000 h^{-1} (GHSV, NTP)] the Thiele modulus was calculated to be 0.082, using k_1 = 0.93/s, effective diffusivity = 0.014 cm^2/s, and pellet radius = 0.03 cm. Under the same conditions, the temperature difference between the bulk gas and the exterior surface of the catalyst was estimated to be only 5.2 K and the temperature difference between the surface and the center of the particle was estimated to be only 0.6 K.

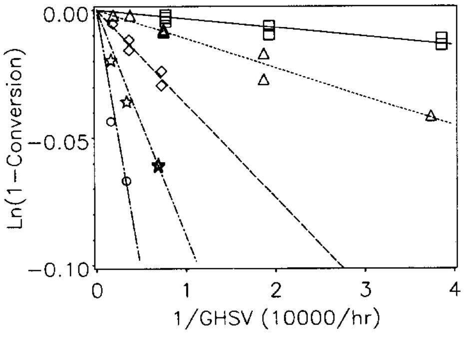

FIG. 3. Rate constant plot based on Eq. (1). (□— 773 K, △--- 798 K, ◇- - - 823 K, ☆— 848 K, ○—— 873 K.)

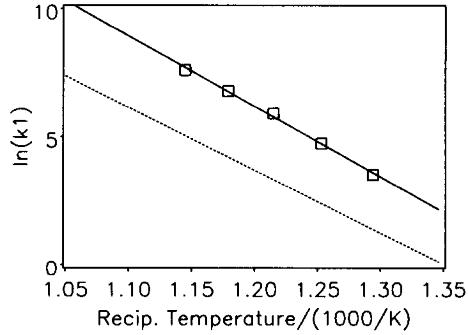

FIG. 4. Arrhenius plot for k_1 [dotted line is for MoO_3–SiO_2 catalyst under similar conditions (*8*)].

A comparison of the observed versus the predicted methane conversion, based on a first-order model, is shown in Fig. 5. There

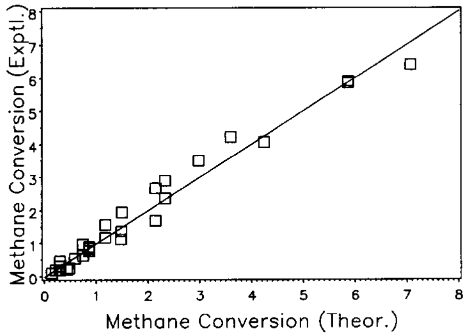

FIG. 5. Comparison of experimental and model-calculated methane conversion.

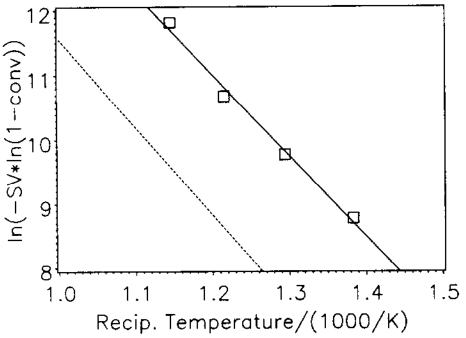

FIG. 6. Arrhenius plot for k_2 [dotted line is for MoO_3–SiO_2 catalyst under similar conditions (*8*)].

TABLE 2

Kinetic Parameters[a]

Index	Reaction	k_i at 873 K (h^{-1})	k_i^0 (h^{-1})	E_i (kJ $mole^{-1}$)
1	$CH_4 \rightarrow HCHO$	2,018 (171)	6.50×10^{16} (3.02×10^{13})	227 (189)
2	$HCHO \rightarrow CO$	129,527 (12,638)	2.00×10^{11} (1.19×10^{12})	104 (134)
3	$CO \rightarrow CO_2$[b]	4,630 (21.13)	1.05×10^{9} (3.73×10^{12})	90.0 (189)

[a] Values in parentheses are for MoO_3–SiO_2 (*8*).

[b] $CH_4 \rightarrow CO_2$ for MoO_3–SiO_2 system.

is good agreement between theory and experiment.

A first-order kinetic rate law was used to describe formaldehyde oxidation (*8, 12*). Thus,

$$\ln\left[-\mathrm{GHSV} \cdot \ln\left(1 - \frac{c_{\mathrm{CO}} + c_{\mathrm{CO_2}}}{c^0_{\mathrm{HCHO}}}\right)\right] = \ln k_2^0 - \frac{E_2}{RT} \quad (2)$$

In Fig. 6, the left-hand side of Eq. (2) is plotted vs $1/T$. The data fall on a straight line and yield k_2^0 and E_2 values.

Assuming that the carbon monoxide oxidation proceeds to carbon dioxide via a first-order reaction (*12*), an analytical expression for the yield of carbon monoxide was derived. This expression was used along with the standard nonlinear parameter estimation method to obtain best-fit values for k_3^0 and E_3. Goldwasser and Trimm (*13*) have measured rates for CO oxidation on V_2O_5–SiO_2 (1 wt% V_2O_5). At 733 K, their reactor-volume-based rate constant of 430 h^{-1} compares well with our (model-derived) k_3 value of 441 h^{-1}, showing that our mechanism is consistent with the previously observed CO oxidation activity of V_2O_5–SiO_2. Values of preexponential factors and activation energies obtained in our study are summarized in Table 2.

Analytical relationships between product selectivities and methane conversion are summarized in Table 3. Selectivities depend on methane conversion and on temperature. Using these selectivity relationships, predicted selectivities are compared with the observed values for formaldehyde (Fig. 7) and carbon monoxide (Fig. 8). As seen in Figs. 7 and 8, the scatter around the "$y = x$" line appears to be due to random error.

The selectivity relationships were also used to draw the lines in Figs. 1a through c, which correspond to the model predictions at each temperature. Formaldehyde selectivities at the highest temperature of 873 K were found to lie below model predictions, presumably due to the onset of other reactions that are not accounted for in our present model. As shown in Fig. 1b, the model predicts that at the lower temperatures, carbon monoxide selectivity should

TABLE 3

Product Selectivity Expressions for Methane Oxidation via a Sequential Pathway

$$S_{\mathrm{HCHO}} = \frac{k_1}{(k_2 - k_1)\Psi}\left[1 - \Psi - (1 - \Psi)^{k_2/k_1}\right]$$

$$S_{\mathrm{CO}} = \frac{k_1 k_2}{(k_3 - k_1)(k_3 - k_2)\Psi}(1 - \Psi)^{k_3/k_1} + \frac{k_1 k_2}{(k_2 - k_1)\Psi}\left[\frac{(1 - \Psi)}{(k_3 - k_1)} - \frac{(1 - \Psi)^{k_2/k_1}}{(k_3 - k_2)}\right]$$

$$S_{\mathrm{CO_2}} = 1 - S_{\mathrm{HCHO}} - S_{\mathrm{CO}}$$

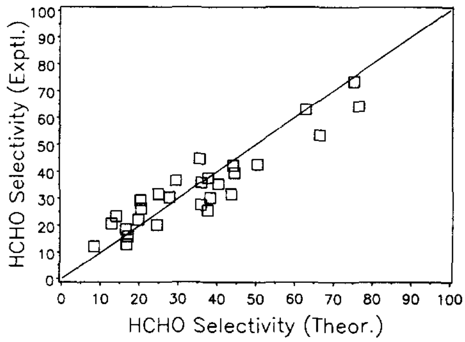

FIG. 7. Comparison of experimental and model-calculated HCHO selectivity.

go through a maximum as conversion is increased. The solid lines in Fig. 2 also represent model predictions. As in the data, the model predicts a maximum in carbon monoxide concentration. Generally, model predictions compare well with the experimental observations.

The mathematical model is built on the assumption that the reaction rate is zero order in oxygen concentration. This assumption should break down when the oxygen concentration becomes very low. This regime was not extensively investigated as the nature of the catalytic surface was thought to change in low oxygen concentrations. The upper limit on the oxygen concentration in the reactant mixture was kept low and well below the explosion limit. The methane conversion was limited by the oxygen present and in no case exceeded 7%. Several of these considerations are similar to those discussed in our previous paper (*8*).

DISCUSSION

V_2O_5–SiO_2 appears to be a highly selective catalyst for HCHO formation from methane at low conversion. However, this system suffers from a rapid falloff in HCHO selectivity as methane conversion increases. Similar behavior was observed by Zhen *et al.* (*5*) using N_2O as an oxidant with a V_2O_5–SiO_2 catalyst. With N_2O, however, methanol was also produced with significant selectivity.

It has previously been reported (*7, 14*) that silica itself appears to catalyze the partial oxidation of methane to formaldehyde. In the present study it appears that less than 0.1 monolayer of V_2O_5 enhances the methane conversion activity of the silica by approximately a factor of 50 at 848 K and 5000 h^{-1} (GHSV, NTP).

Comparison of V_2O_5–SiO_2 and MoO_3–SiO_2 Catalysts

The dotted lines in the Arrhenius plots (Figs. 4 and 6) correspond to data obtained for the MoO_3–SiO_2 catalyst. Preexponential factors and activation energies for the MoO_3–SiO_2 system are summarized in parentheses in Table 2. The V_2O_5–SiO_2 catalyst has a much higher oxidation activity than MoO_3–SiO_2. This was also observed when N_2O was used as an oxidant (*4, 5*).

To illustrate the differences in mechanism between the two catalysts, the formaldehyde and carbon dioxide selectivities for the MoO_3–SiO_2 catalyst are reproduced from (*8*) as Figs. 9a and b. Selectivity to carbon dioxide for the V_2O_5–SiO_2 system is zero at low methane conversions (Fig. 1c), while for the MoO_3–SiO_2 system it is independent of conversion at ≈11% (Fig. 9b). Formaldehyde is the only primary product in the V_2O_5–SiO_2 system, in contrast to MoO_3–SiO_2, where both formaldehyde and

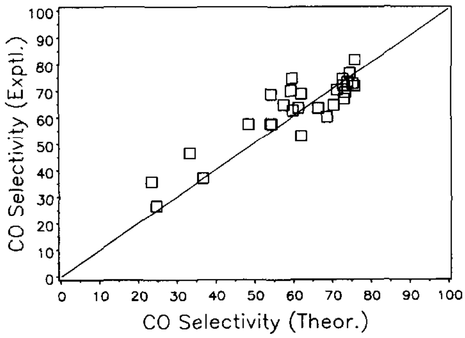

FIG. 8. Comparison of experimental and model-calculated CO selectivity.

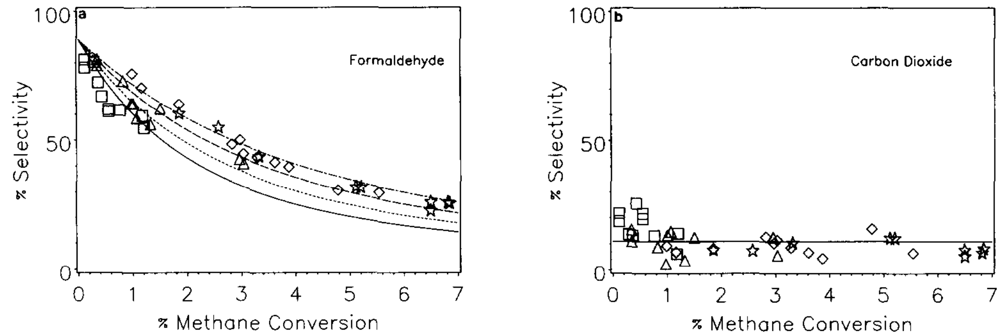

FIG. 9. Selectivity vs methane conversion curves for MoO_3–SiO_2 catalyst. Symbols correspond to data; lines correspond to model predictions (□— 848 K, △ --- 873 K, ◇—– 898 K, ☆—– 923 K).

carbon dioxide are formed directly from methane via parallel pathways. Both catalyst systems oxidize formaldehyde to carbon monoxide, but the MoO_3–SiO_2 catalyst appears to be much less active than V_2O_5–SiO_2 for the conversion of CO to CO_2. This is consistent with the work of Nozaki and Ohki (*15*) where, in the range 723–823 K, unsupported V_2O_5 was found to be more active than MoO_3 for CO oxidation.

The effect of temperature (at constant conversion) on HCHO selectivity appears to be much more marked for V_2O_5–SiO_2 (Fig. 1a) than in the MoO_3–SiO_2 case (Fig. 9a). The larger temperature dependence is a result of the greater difference in activation energies for the HCHO formation and destruction reactions (Table 2). Overall, despite the high activity of the V_2O_5–SiO_2 catalysts, HCHO yields at a given methane conversion are lower than in the MoO_3–SiO_2 system (Fig. 10).

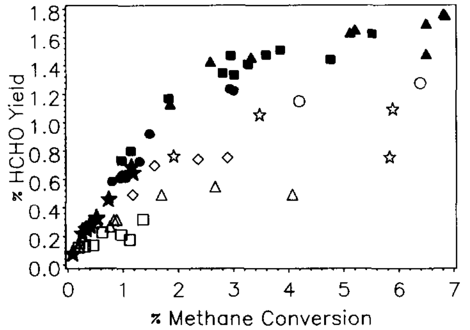

FIG. 10. Comparison of formaldehyde yield as a function of methane conversion for V_2O_5–SiO_2 (□ 773 K, △ 798 K, ◇ 823 K, ☆ 848 K, ○ 873 K) and MoO_3–SiO_2 (★ 848 K, ● 873 K, ■ 898 K, ▲ 923 K) catalysts.

MoO_3–SiO_2 and V_2O_5–SiO_2 are the only catalyst systems studied so far that display such high selectivities to formaldehyde in the presence of molecular oxygen. It is interesting to note that, like MoO_3, V_2O_5 has a tendency to form reduced, edge-sharing shear structures (*16*), suggesting that this facile mode of partial reduction may be an important component in the catalytic mechanism. Also, as with the MoO_3–SiO_2 system, the methane oxidation activity of V_2O_5–SiO_2 is severely poisoned by sodium (*17*). This suggests that, in both cases, the shearing mechanism is being "locked" by the formation of an –ONa unit. This prevents the elimination of water and thereby the reduction of the oxide.

SUMMARY AND CONCLUSIONS

Vanadia–silica is a selective catalyst for the partial oxidation of methane to formaldehyde at low methane conversions. As methane conversion increases, formaldehyde selectivity decreases. At a fixed methane conversion, formaldehyde selectivity can be increased by increasing temperature.

Kinetic analysis indicates that the methane is directly oxidized to formaldehyde, with formaldehyde being oxidized to carbon monoxide, and carbon monoxide being further oxidized to carbon dioxide. The reactions were all found to be zero order in oxygen concentration. Methane, formaldehyde, and carbon monoxide oxidation were modeled following overall first-order kinetic rate laws. Kinetic constants have been determined and there is good agreement between model predictions and experimental data.

The vanadia–silica catalyst is clearly more active than the molybdena–silica system, although on V_2O_5–SiO_2, selectivity to formaldehyde appears to fall off more rapidly with conversion at all but the highest temperatures investigated. The temperature dependence is different in the two systems, with formaldehyde selectivity varying much more strongly with temperature (at a given conversion) in the V_2O_5–SiO_2 case. A significant difference between the two catalysts is that unlike its molybdena counterpart, which forms HCHO and CO_2 by parallel reaction pathways, vanadia–silica catalyzes the formation of CO_2 via a sequential mechanism.

APPENDIX: NOMENCLATURE

c	mole fraction, mol/total mol
E	activation energy, J/mol
GHSV	gas hourly space velocity, m^3 gas/h · m^3 catalyst
k	rate constant, h^{-1}
R	gas constant, J/mol · K
S	selectivity, mole fraction of total oxidized products
Ψ	mole fractional conversion of methane

Superscript

0	initial value

Subscript

i	index

ACKNOWLEDGMENTS

The authors are very grateful to Carole C. Carey for her skillful experimental work and to Dr. Robert Grasselli and Dr. Michael Wax for many useful discussions.

REFERENCES

1. Van Hook, J. P., *Catal. Rev. Sci. Eng.* **21,** 1 (1980).

2. Klier, K., *Adv. Catal.* **31,** 243 (1982).

3. Machiels, C. J., Chowdhry, U., Staley, R. H., Ohuchi, F., and Sleight, A. W., *in* "Catal. Convers. Synth. Gas Alcohols Chem. (Proc. Symp.)" (R. G. Herman, Ed.), p. 413. Plenum, New York, 1984.

4. Khan, M. M., and Somorjai, G. A., *J. Catal.* **91,** 263 (1985).

5. Zhen, K. J., Khan, M. M., Mak, C. H., Lewis, K. B., and Somorjai, G. A., *J. Catal.* **94,** 501 (1985).

6. Iwamoto, M., *Japan. Kokai Tokkyo Koho,* JP 58-92630 (1983).

7. Spencer, N. D., *J. Catal.* **109,** 187 (1988).

8. Spencer, N. D., and Pereira, C. J., *AIChE J.* **33,** 1808 (1987).

9. Imre, L., and Nassenstein, H., *German Offen.* 2,404,738 (1975).

10. Monnier, J. R., and Keulks, G. W., *Prepr. Amer. Chem. Soc. Div. Petrol. Chem.* **24,** 1 (1979).

11. Grasselli, R. K., and Suresh, D. D., *J. Catal.* **25,** 273 (1972).

12. Golodets, G. I., "Heterogeneous Catalytic Reactions Involving Molecular Oxygen." Elsevier, Amsterdam, 1983.

13. Goldwasser, M. R., and Trimm, D. L., *Ind. Eng. Chem. Prod. Res. Dev.* **18,** 27 (1979).

14. Kasztelan, S., and Moffat, J. B., *J. Chem. Soc. Chem. Commun.,* 1663 (1987).

15. Nozaki, F., and Ohki, K., *Bull. Chem. Soc. Japan* **45,** 3473 (1972).

16. Wells, A. F., "Structural Inorganic Chemistry." Clarendon, Oxford, 1984.

17. Pereira, C. J., and Spencer, N. D., in preparation.